Cell Reports Methods, Volume *1*

Supplemental information

A molecular toolbox

for ADP-ribosyl binding proteins

Sven T. Sowa, Albert Galera-Prat, Sarah Wazir, Heli I. Alanen, Mirko M. Maksimainen, and Lari Lehtiö

Content

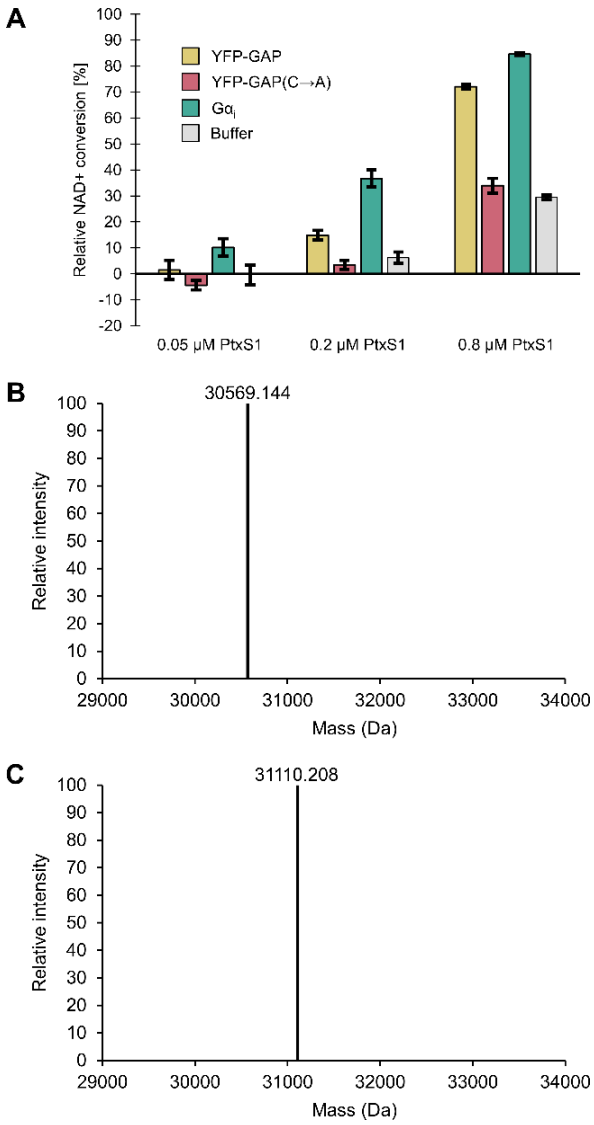

Figure S1. Modification of YFP-GAP by PtxS1, Related to Figure 2. (A) NAD^+ consumption assay. PtxS1 (0.05 µM, 0.2 µM or 0.8 µM) was mixed with 30 µM NAD^+ and 20 µM YFP-GAP, YFP-GAP(C→A), full length $G\alpha_i$ or buffer. Samples were incubated for 1 hour at room temperature. Data shown are mean ± standard deviation with number of replicates n = 4. Analysis of the modification by mass spectrometry: The deconvoluted monoisotopic mass spectra are shown for YFP-GAP (B) before and (C) after ADP-ribosylation with PtxS1 and subsequent purification. The mass difference is 541.064 Da and corresponds to the theoretical monoisotopic mass of a single ADP-ribosyl group (541.061 Da).

The NAD^+ consumption assay for PtxS1 was performed as previously described (Ashok et al., 2020). All incubation steps were performed at room temperature. Briefly, reactions were mixed and 10 µl per well transferred to a black polypropylene low-volume 384-well plate (FisherBrand) and incubated for 1 h. Samples containing no PtxS1 were used to calculate the relative conversion. Unreacted NAD^+ was converted to a fluorescent product by addition of 4 µl 2 M KOH and 4 µl 20%(v/v) acetophenone in ethanol. After incubation for 10 minutes, 18 µl formic acid per well was added and reactions were incubated for 30 minutes. Fluorescence was measure using Tecan M1000 Pro multimode plate reader. The samples were excited at 372 nm wavelength and emission at 444 nm wavelength was measured.

For analysis by mass spectrometry, YFP-GAP or YFP-GAP(MAR) (50 µM) was mixed with 0.1% trifluoracetic acid. The molecular weights of purified protein samples were measured by electrospray ionization mass spectrometry combined with liquid chromatography (LC-ESI-MS) using a Q Exactive Plus Mass Spectrometer.

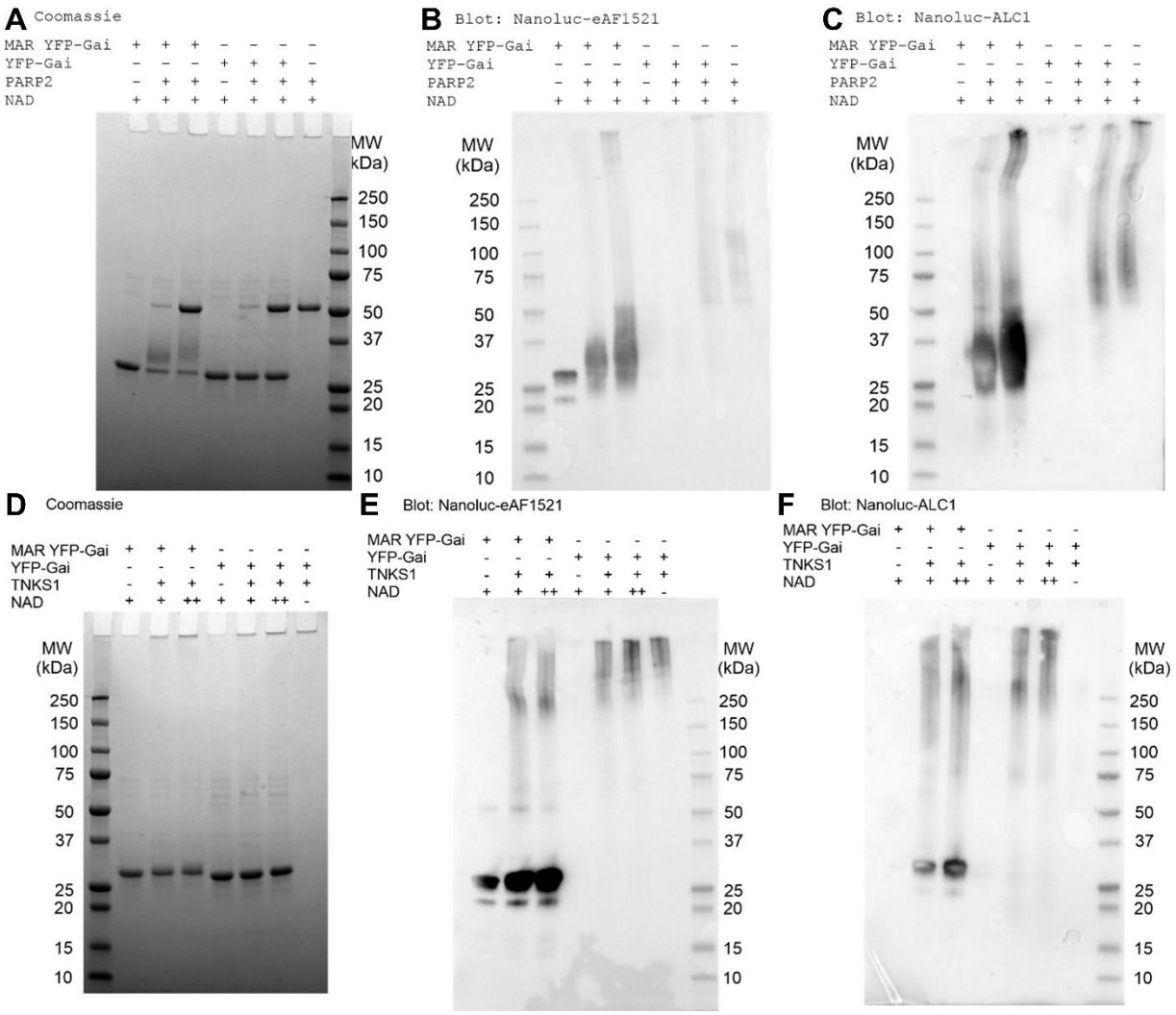

Figure S2. PARylation of MARylated YFP-GAP with PARP2 or TNKS1, Related to Figure 2. PARylation with PARP2: Full gel and blots of those shown in figure 2b. Samples were analysed by SDS-PAGE and coomassie staining (A), as well as with western blot using nanoLuc-eAf1521 (B) or nanoLuc-ALC1 (C). PARylation with TNKS1: 200 nM TNKS1 (SAM-Catalytic domain dimer) was mixed with YFP-GAP or YFP-GAP(MAR) and incubated overnight at room temperature in the presence of 1 mM (+) or 10 mM (++) NAD^+. Samples were analysed by SDS-PAGE and coomassie staining (D), as well as with western blot using nanoLuc-eAf1521 (E) or nanoLuc-ALC1 (F).

Dimeric TNKS1 was formed by incubating 2 independently purified samples consisting of TNKS1 SAM-Catalytic domain containing mutations E1050K and Y1073A in SAM domain. Incubation of YFP-GAP is MARylated with TNKS1 dimer results in a change in electrophoretic mobility (Figure S2D). The PARylation of YFP-GAP requires the protein to be previously MARylated suggesting that only one PAR chain is added to the YFP-GAP in extending the MAR modification. Since ALC1 detects only PAR chains, the blot in Figure S2F indicates that the modification formed corresponds to a PAR polymer.

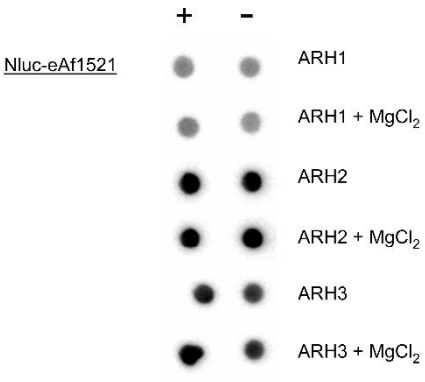

Figure S3. Hydrolysis test of cysteine-ADP-ribose with ARH family members, Related to Figure 4. YFP-GAP(MAR) (10 µM) was incubated in presence (+) or absence (-) of 1 µM CFP-fused ARH constructs. The reactions were prepared in the presence of absence of 5 mM $MgCl_2$, incubated for 24 h at room temperature and thereafter blotted on nitrocellulose membranes. The membranes were washed and the protein-bound ADP-ribosyl-groups detected using Nluc-eAf1521.

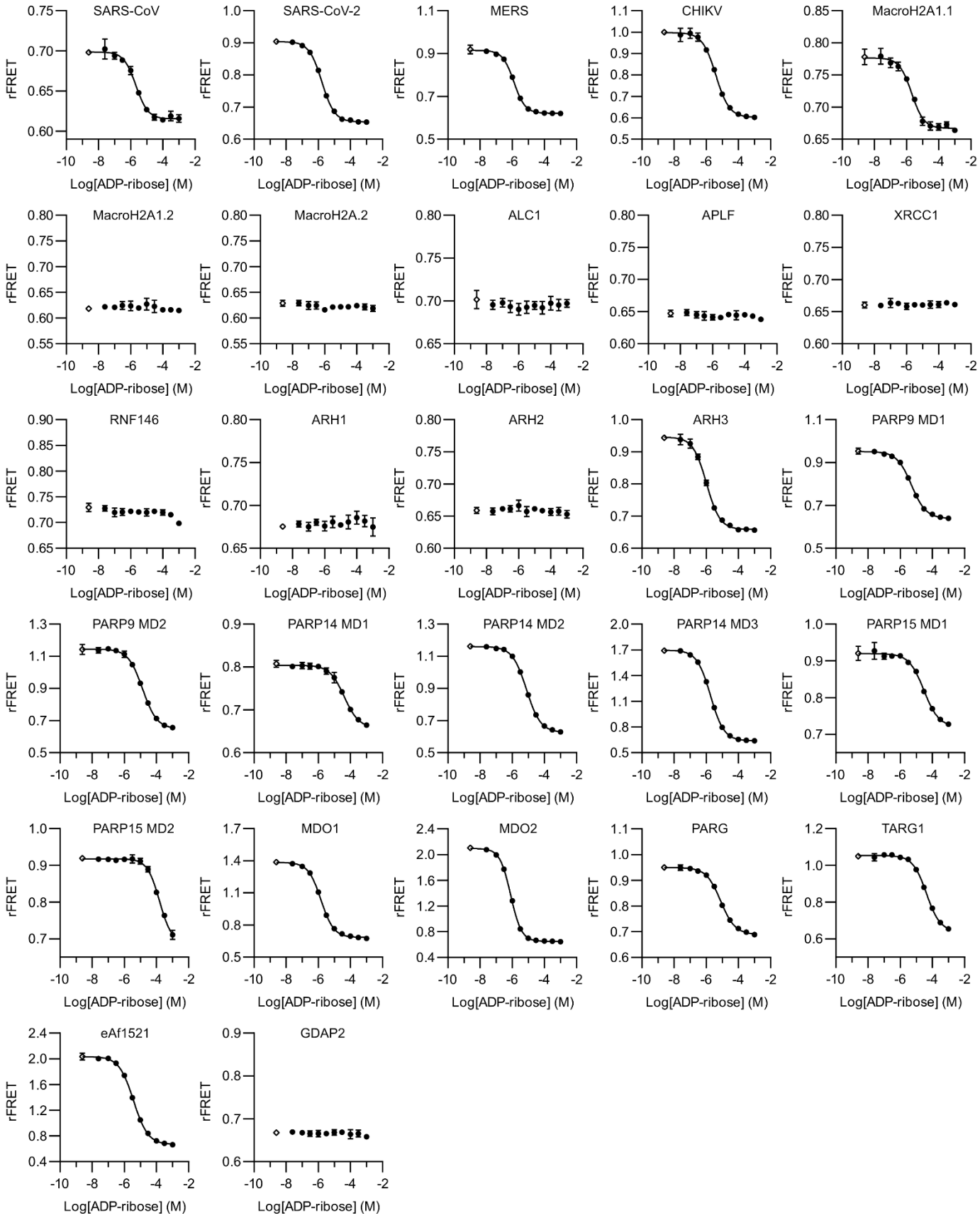

Figure S4. ADP-ribose dose-response curves for CFP-fusion constructs and MARylated YFP-GAP, Related to Figure 4. CFP-fused constructs (1 µM) were mixed with YFP-GAP(MAR) (5 µM) and increasing concentrations of ADP-ribose. The ratiometric FRET signals (rFRET) were determined. Data shown are mean ± standard deviation with number of replicates n = 4. The controls containing no ADP-ribose were set one logarithmic unit below the lowest concentration.

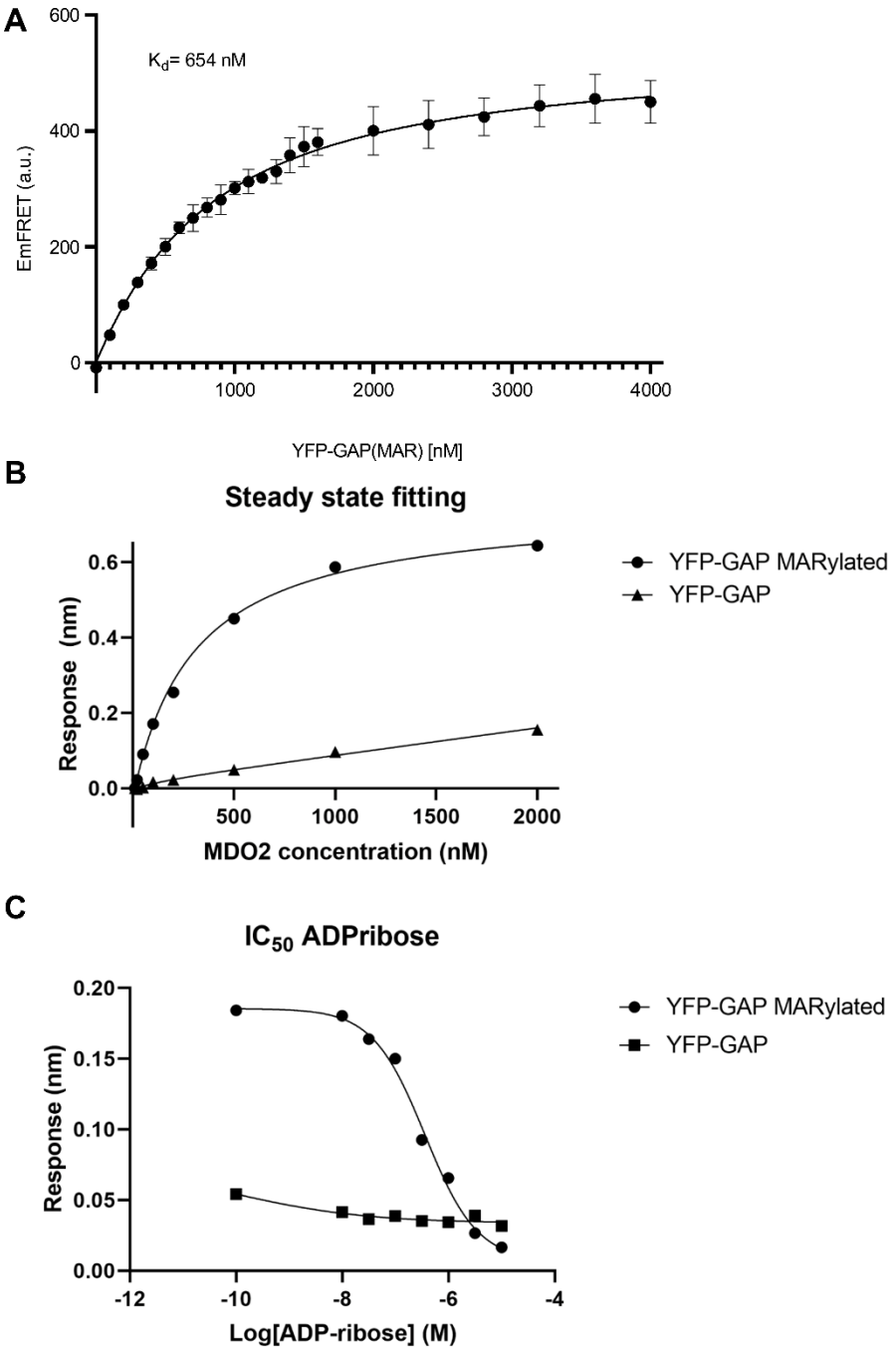

Figure S5. Determination of binding affinity for CFP-MDO2 and YFP-GAP(MAR) by FRET and BLI, Related to Figure 5. (A) FRET-based determination of the binding affinity. CFP-MDO2 (290 µM) was mixed with increasing concentrations of YFP-GAP(MAR). Determination of the binding affinity was done as previously described (Sowa et al., 2020). Equations for calculation of the FRET emission (EmFRET) and mathematical fit were used as previously described (Song et al., 2012). Data shown are mean ± standard deviation with number of replicates n = 4. (B) Affinity of MDO2 for YFP-GAP(MAR) loaded sensors. Steady state signal is plotted against MDO2 concentration in solution. K_D 500 ±120 nM for YFP-GAP(MAR) loaded sensor was determined with single exponential fit to 3 independent experiments. Individual values represent the average ± SD response during last 20 seconds of the association step. (C) IC_{50} determination of ADP-ribose with MDO2. MDO2 concentration was kept constant at 100 nM and ADP-ribose concentration was varied between 10 µM to 10 nM. IC_{50} determined for YFP-GAP MARylated is 440 nM (pIC_{50}=6.36 ± 0.08) from 3 independent experiments. Individual values represent the average ± SD response during last 20 seconds of the association step.

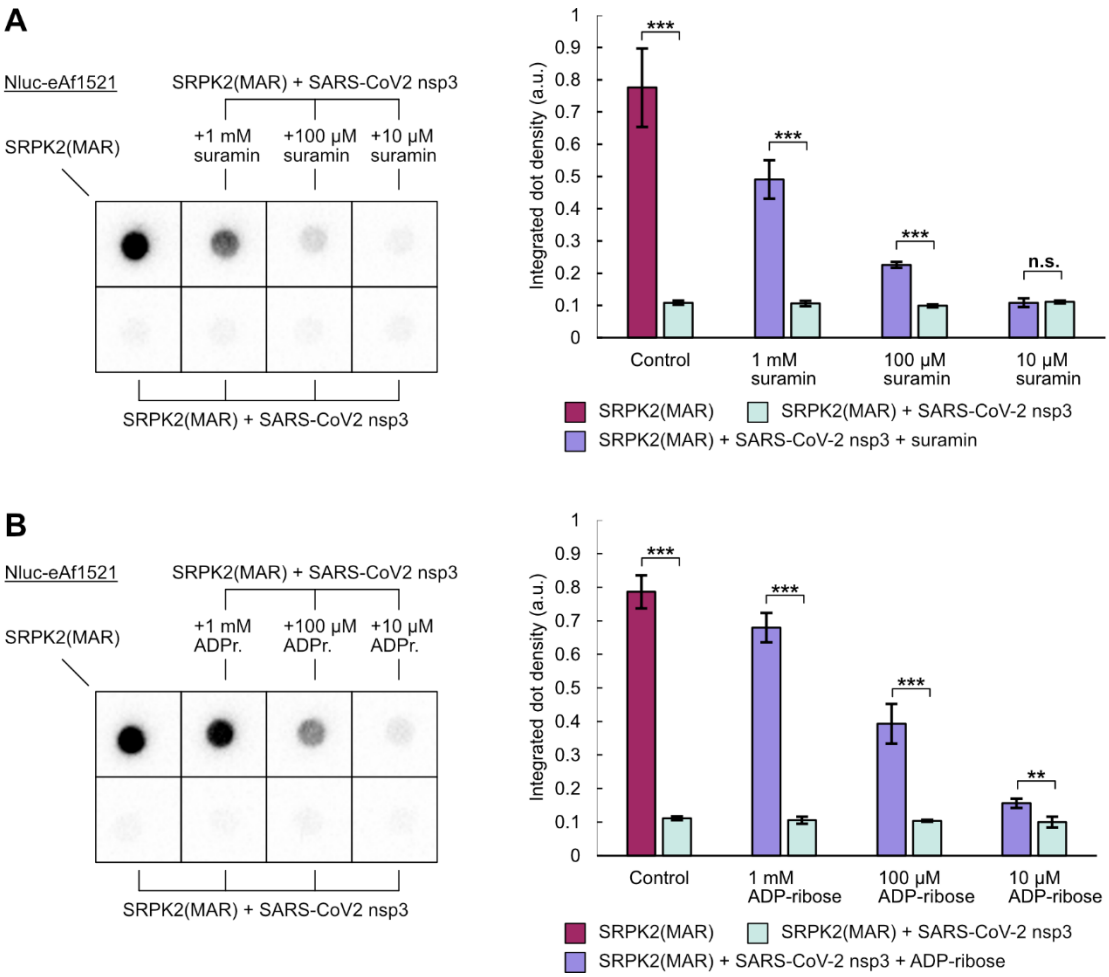

Figure S6. Inhibition of the hydrolytic activity of the SARS-CoV-2 nsp3 macrodomain by suramin and ADP-ribose, Related to Figure 6. MARylated SRPK2 (2 µM) was mixed with 100 nM of CFP-fused SARS-CoV-2 nsp3 macrodomain and incubated for 4 h at room temperature in the absence or presence of (A) suramin or (B) ADP-ribose. Controls containing only MARylated SRPK2 (2 µM) were prepared. Nluc-eAf1521 was used to detect the protein-bound mono-ADP-ribosyl groups. Representative dot blots are shown. In total, four dots of each condition shown were blotted from the same reaction well to the membrane to evaluate blotting accuracy and dot intensities were determined. Data shown are mean ± standard deviation with number of replicates n = 4 (unpaired t-test: n.s. $p > 0.05$; *$p < 0.05$; **$p < 0.01$; ***$p < 0.001$.).

To prepare MARylated SRPK2, His_6-tagged SRPK2 (10 µM) were mixed with 5 µM PARP10 and 20 µM NAD^+ in reaction buffer (50 mM Tris pH 7.2) and let incubate for 1 h at room temperature. An additional 6.7 µM NAD^+ and 1 µM PARP10 were added. The reaction was incubated for 1.5 h at room temperature. The MARylated SRPK2 was purified by IMAC on a 1 ml HiTrap IMAC HP column charged with Ni^{2+} and buffer exchanged to 30 mM HEPES pH 7.5, 500 mM NaCl, 0.5 mM TCEP. Reactions containing 2 µM MARylated SRPK2 and 100 nM CFP-fused SARS-CoV-2 nsp3 macrodomain in the absence or presence of suramin or ADP-ribose were prepared in Echo source plates in 25 mM HEPES pH 7.5 and incubated for 4 h at room temperature. Per reaction condition, four dots (0.5 µl each) were transferred to the membrane using an Echo 650 device. The membrane was prepared using 0.1 µg/ml Nluc-eAf1521 as described in the method section. For detection, 500 µl of 10 mM sodium phosphate (pH 7.0) containing 1 M NaCl and 1:250 NanoGlo substrate were transferred to the membrane. The blot was imaged and the dot intensities were calculated as integrated densities with ImageJ (Schneider et al., 2012) using a MicroArray profile plugin (OptiNav).